

CHAPTER IV

RESULTS AND DISCUSSION

4.1. The Effect of Operating Parameters and Determination of Kinetics of the Reaction at Atmospheric Pressure

For this experiment, the elementary reaction rate with order of reaction for methane and steam could be expressed in rate equation as follows:

$$-r_{\text{CH}_4} = k P_{\text{CH}_4}^m P_{\text{H}_2\text{O}}^n \quad (4.1)$$

Where $-r_{\text{CH}_4}$ = reaction rate of methane, which was defined in equation (4.2)

k = rate constant

P_{CH_4} = partial pressure of methane (atm)

$P_{\text{H}_2\text{O}}$ = partial pressure of steam (atm)

m, n = order of reaction for methane and steam, respectively

Also, reaction rate of methane could be defined to the ratio of methane conversion with proportion between catalyst weight and methane feed rate as follows:

$$-r_{\text{CH}_4} = \Delta X_{\text{CH}_4} / (W/F_{\text{CH}_4}) \quad (4.2)$$

Where ΔX_{CH_4} = methane conversion

W = catalyst weight

F_{CH_4} = methane feed rate

4.1.1. Excess Steam Condition

The objective of this part was to study rate of reaction and the effect on methane conversion at excess steam. The experiment was achieved at 700-850 °C, excess steam to methane ratio, 6.0×10^{-5} to 6.0×10^{-4} mole/min of methane feed rate, 0.15 mole/min of steam feed rate and 2 g of catalyst weight. Owing to excess steam, order of reaction for steam was no effect on reaction rate of methane that rate equation in equation (4.1) could be rearranged as follows:

$$-r_{\text{CH}_4} = k P_{\text{CH}_4}^m \quad (4.3)$$

From the experimental result, Table C1 in Appendix C, Figure 4.1 showed plot between methane conversion and ratio of catalyst weight with methane feed rate at several temperatures. Methane conversion increased with elevated temperature and mostly closed to equilibrium at 850 °C because steam reforming was strongly endothermic reaction. Moreover, methane conversion also increased with decreasing methane feed rate due to the increase of contact time.

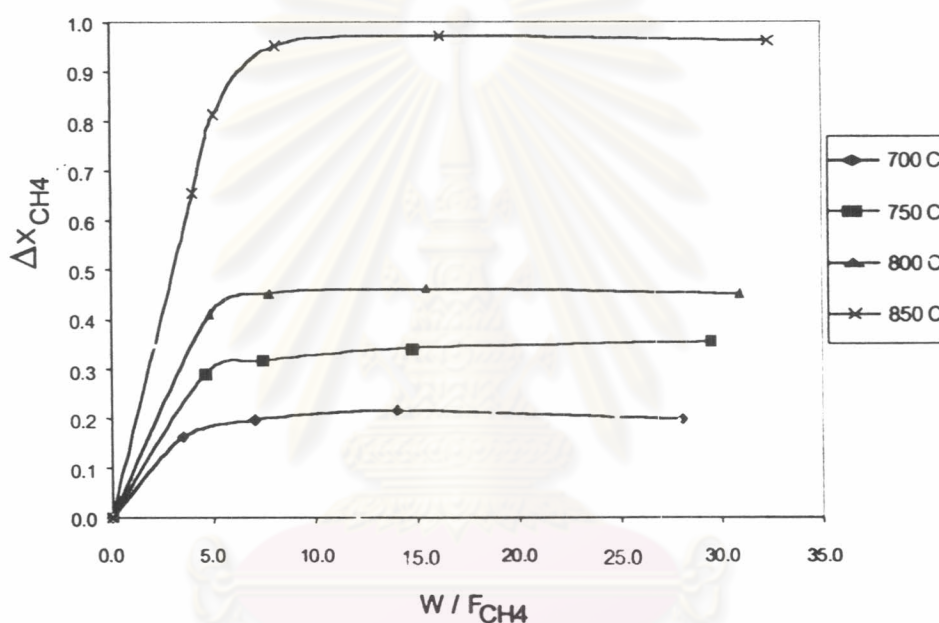


Figure 4.1. ΔX_{CH_4} vs. W/F_{CH_4} at several temperatures.

From equation (4.3), which could be rearranged as follows:

$$\ln(-r_{\text{CH}_4}) = \ln k + m \ln(P_{\text{CH}_4}) \quad (4.4)$$

Then, both rate constant (k) and order of reaction for methane (m) could be given with plot between $\ln(-r_{\text{CH}_4})$ and $\ln(P_{\text{CH}_4})$ at several temperatures, which was illustrated in Figure 4.2. It was found that rate constant increased with elevated temperature whereas order of reaction for methane was quite similar with close to one. Thereafter, activation energy (E_a) was considered with the Arrhenius law as follows:

$$k = k_0 \exp(-E_a/RT) \quad (4.5)$$

$$\ln k = \ln k_0 - E_a/RT \quad (4.6)$$

From equation (4.6), activation energy could be given with plot between $\ln k$ and $(1/T)$, which was illustrated in Figure 4.3. Thus, values of rate constant, order of reaction for methane, and activation energy were indicated in Table 4.1.

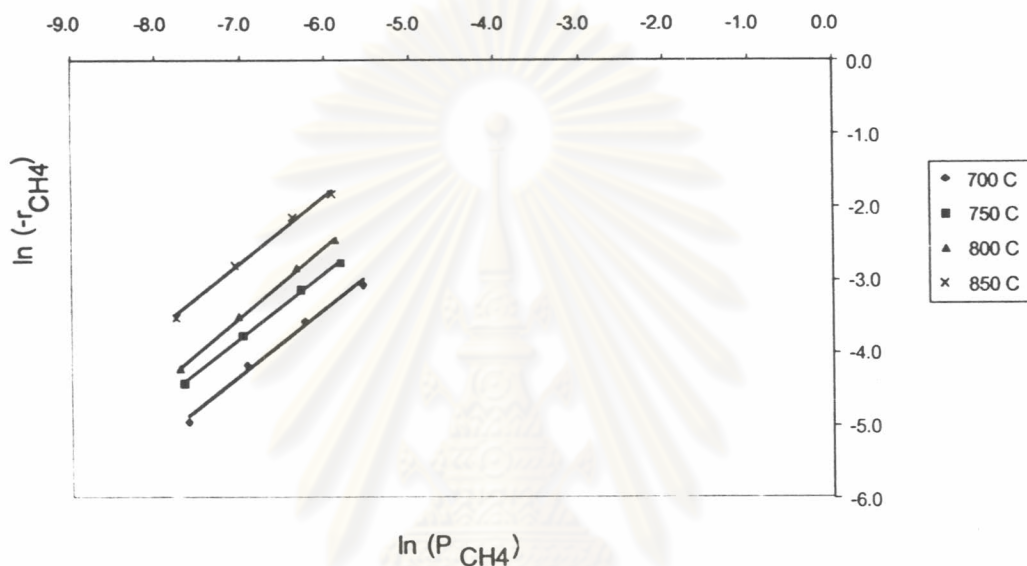


Figure 4.2. $\ln(-r_{CH_4})$ vs. $\ln(P_{CH_4})$ at several temperatures.

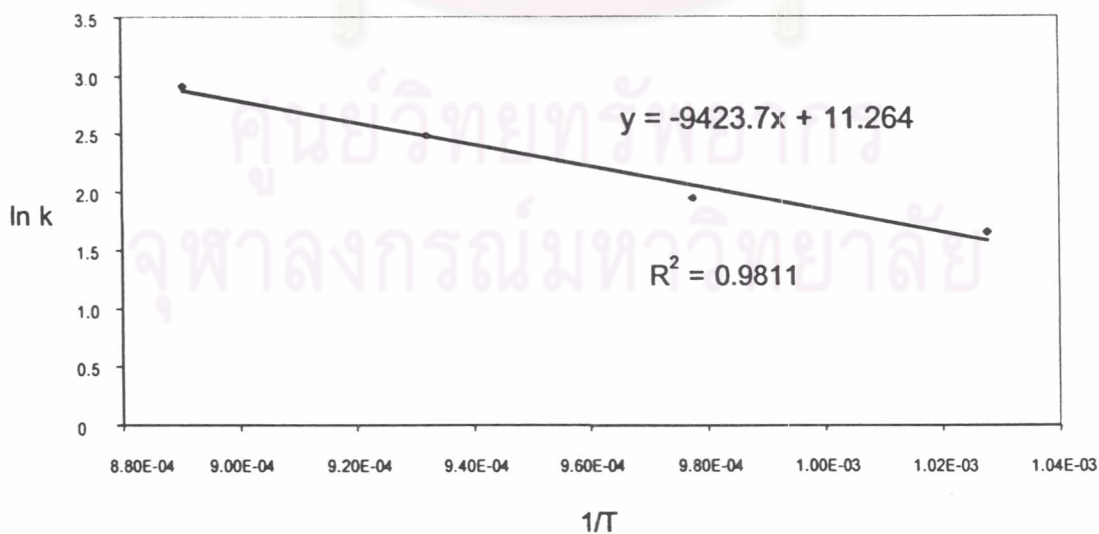


Figure 4.3. $\ln k$ vs. $(1/T)$ at excess steam.

Table 4.1. Values of rate constant, order of reaction for methane and activation energy.

Reaction Temperature (°C)	1/T	ln k	k	CH ₄ Order	ln k _o	k _o	-Ea/R	Ea (cal/mole)
700	1.03E-03	1.6466	5.1893	0.9080	11.264	7.796E+04	-9423.7	18,726.78
750	9.78E-04	1.9430	6.9797	0.8918				
800	9.32E-04	2.4854	12.0059	0.9567				
850	8.90E-04	2.9094	18.3458	0.9235				

From Table 4.1, the rate equation of methane steam reforming at excess steam could be expressed as follows:

$$-r_{\text{CH}_4} = k P_{\text{CH}_4} \quad (4.7)$$

Where $k = 7.796 \times 10^4 \exp(-18,726.78 / RT)$ mole atm⁻¹ kg⁻¹ min⁻¹

4.1.2. Non-Excess Steam Condition

The objective of this part was to study rate of reaction and the effect on methane conversion at non-excess steam. The experiment was divided into two parts. First part was to study the effect on methane conversion at 850 °C, steam to methane ratio from 2.0 to 8.0, methane feed rate from 6.0×10^{-5} to 5.1×10^{-4} mole/min, steam feed rate from 1.0×10^{-4} to 4.1×10^{-3} mole/min and 2 g of catalyst weight. The second part was to study rate of reaction at 700-850 °C, steam to methane ratio from 2.0 to 8.0, 1.0×10^{-3} to 1.25×10^{-3} mole/min of methane feed rate, 2.0×10^{-3} to 1.0×10^{-2} mole/min of steam feed rate and 2 g of catalyst weight. Owing to non-excess steam, order of reaction for methane and steam had effect on reaction rate of methane that rate equation could be also expressed as equation (4.1) as follows:

$$-r_{\text{CH}_4} = k P_{\text{CH}_4}^m P_{\text{H}_2\text{O}}^n$$

Which could be rearranged as follows:

$$\ln(-r_{\text{CH}_4}) = \ln k + m \ln(P_{\text{CH}_4}) + n \ln(P_{\text{H}_2\text{O}}) \quad (4.8)$$

From the experimental result, Table C3 in Appendix C, Figure 4.4 showed plot between methane conversion and ratio of catalyst weight with methane feed rate at several steam-methane ratios. Methane conversion increased with increasing steam-methane ratio and mostly closed to equilibrium at ratio of 8.0 because the equilibrium of steam reforming was shifted to the increase of product gas. In addition, methane conversion also increased with decreasing methane and steam feed rate due to the increase of contact time.

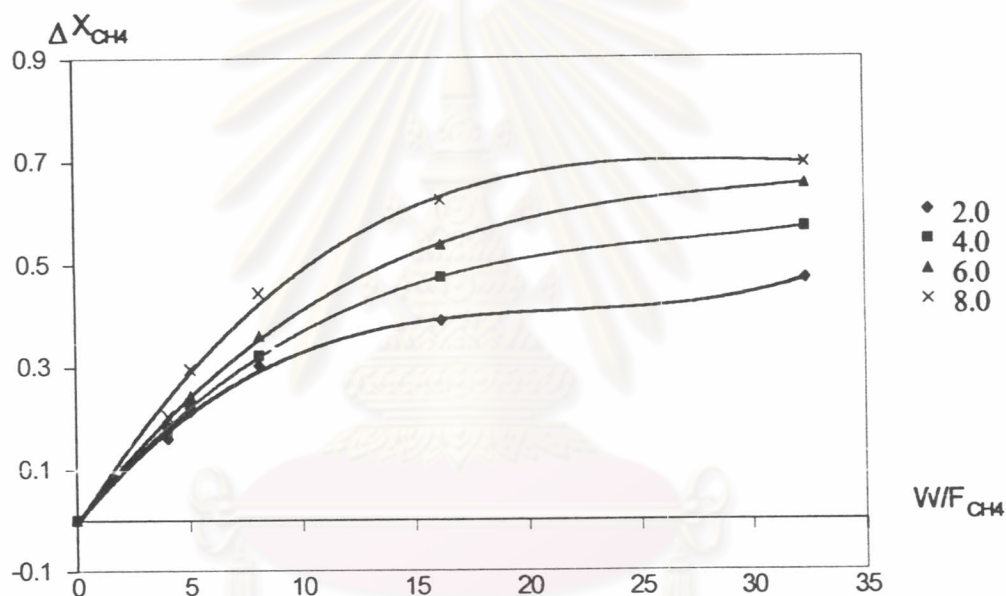


Figure 4.4. ΔX_{CH_4} vs. W/F_{CH_4} at several steam-methane ratios.

From equation (4.8), both rate constant (k) and order of reaction for methane (m) and steam (n) could be given by using multiple linear regression method, which depended on the experimental data from Table C2 (Appendix C). It was found that rate constant increased with elevated temperature, besides, order of reaction for methane was close to one whereas order of reaction for steam was close to one-half. Thereafter, activation energy (E_a) was considered with plot between $\ln k$ and $(1/T)$ as illustrated in Figure 4.5. Thus, values of rate constant, order of reaction for methane and steam, and activation energy were indicated in Table 4.2.

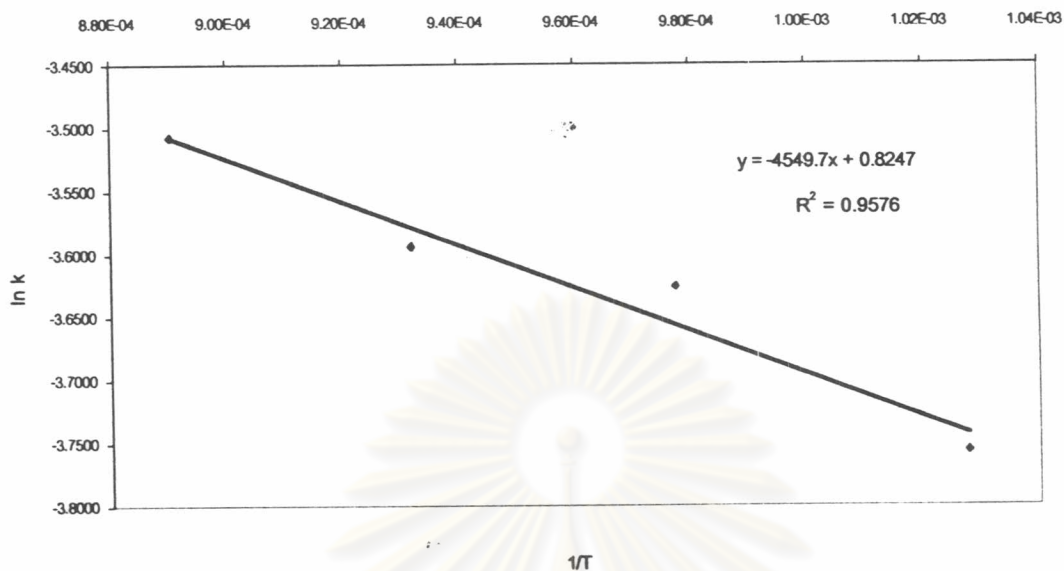


Figure 4.5. $\ln k$ vs. $(1/T)$ at non-excess steam.

Table 4.2. Values of rate constant, order of reaction for methane and steam, and activation energy.

Reaction Temperature (°C)	1/T	ln k	k	CH ₄ Order	H ₂ O Order	ln k ₀	k ₀	-Ea/R	Ea (cal/mole)
700	1.03E-03	-3.7565	0.02337	0.9128	0.4413	0.8247	2.2812	-4549.7	9,041.16
750	9.78E-04	-3.6260	0.02662	0.9776	0.4357				
800	9.32E-04	-3.5938	0.02749	0.9331	0.4224				
850	8.90E-04	-3.5072	0.02998	0.9519	0.4157				

From Table 4.2, the rate equation of methane steam reforming at non-excess steam could be expressed as follows:

$$-r_{\text{CH}_4} = k P_{\text{CH}_4} P_{\text{H}_2\text{O}}^{0.5} \quad (4.9)$$

Where $k = 2.2812 \exp(-9,041.16 / RT)$ mole atm^{-1.5} kg⁻¹ min⁻¹

4.1.3. The Effect of Catalyst Weight

The objective of this part was determination of the optimum catalyst weight on methane conversion, hydrogen-carbon monoxide ratio and product gas composition at 850 °C, excess steam to methane ratio, 1.27×10^{-4} mole/min of methane feed rate and 0.15 mole/min of steam feed rate. The catalyst weight was varied from 2, 5, 8 and 10 g. From the experimental result, Table C7 in Appendix C, Figure 4.6 showed methane conversion increased with increasing catalyst weight and mostly close to equilibrium at 10 g of catalyst weight as reactant could contact with catalyst for a long time and also increased active sites of catalyst to occur reaction increasingly. In addition, hydrogen-carbon monoxide ratio decreased with increasing catalyst weight as illustrated in Figure 4.7. Figure 4.8 showed amount of product gas composition, it was found that hydrogen increased from 77.15 % to 86.20 %, carbon monoxide increased a little from 12.66 % to 13.05 %, carbon dioxide decreased from 3.59 % to 0.26 % and unconverted methane decreased from 6.60 % to 0.50 % with increasing catalyst weight. However, the catalyst weight had no effect on hydrogen-carbon monoxide ratio because product gas composition was dependent on temperature and steam-methane ratio only. Besides, if below 2 g of catalyst weight, the reaction would be occurred a little due to decreasing active sites of catalyst, but if above 10 g of catalyst weight, the reaction rate would be slow because contact time was too increased. Then, the optimum catalyst weight showed the best rate of reaction and the most occurring of reaction.

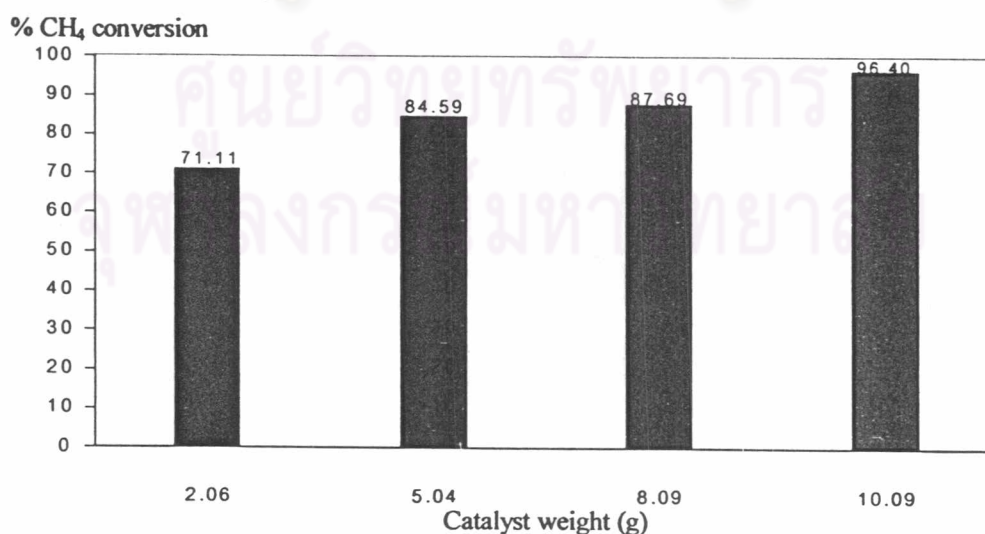


Figure 4.6. Methane conversion vs. catalyst weight.

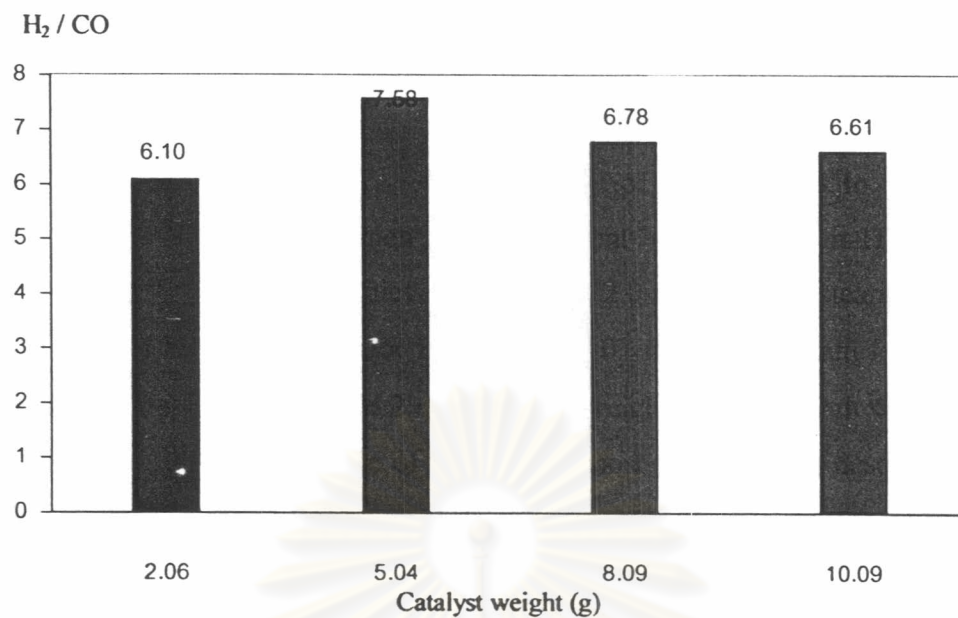


Figure 4.7. Hydrogen-carbon monoxide ratio vs. catalyst weight.

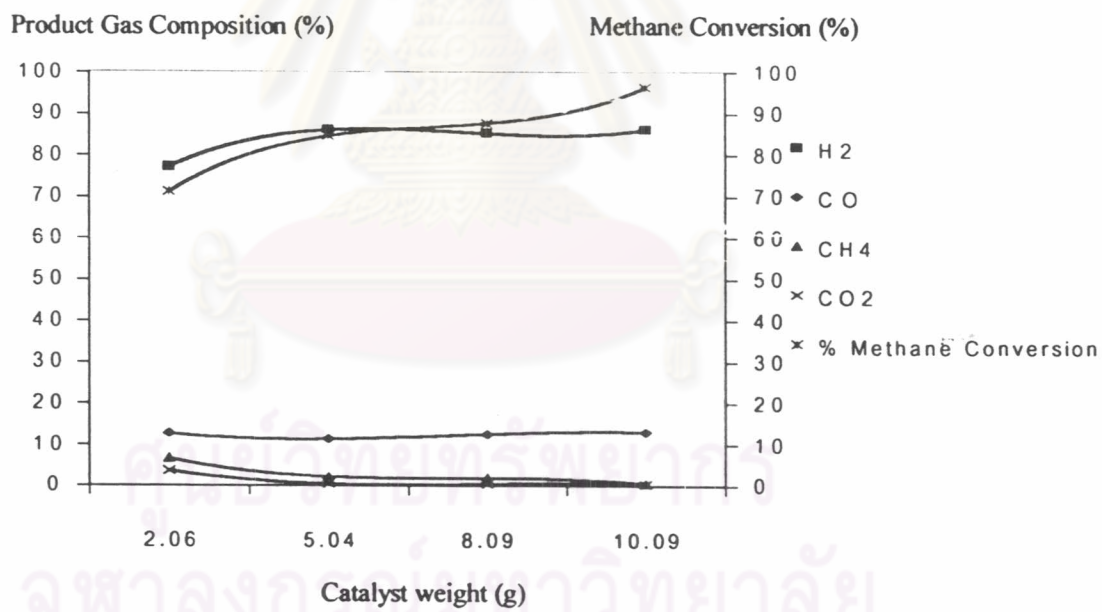
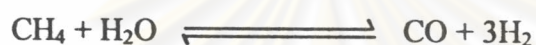


Figure 4.8. Product gas composition and methane conversion vs. catalyst weight.

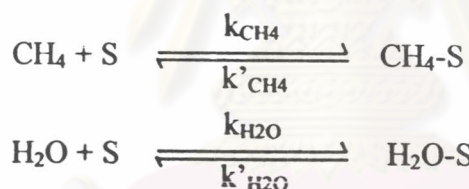
4.2. Reaction Mechanism and Determination of Rate Equation by Langmuir-Hinshelwood Model

The objective of this part was to study the mechanism and rate of reaction, which was consistent with Langmuir-Hinshelwood model. The experiment was achieved at 850 °C, 2.0 to excess of steam to methane ratio, methane feed rate from 6.0×10^{-5} to 5.1×10^{-4} mole/min, steam feed rate from 1.27×10^{-4} to 0.15 mole/min and 2 g of catalyst weight. This research was to study methane steam reforming, then one of the method most often used to describe this catalytic reaction mechanism was the Langmuir-Hinshelwood model. The reaction of methane steam reforming was as follows:

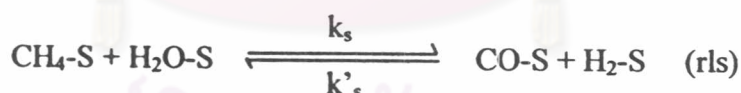


The mechanism of steam reforming could be written as a series of elementary steps as follows:

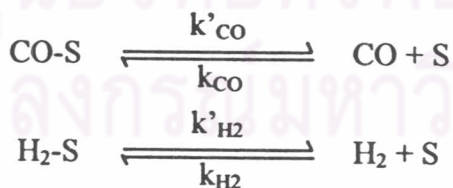
1. Adsorption



2. Surface reaction



3. Desorption



Where

S = Active sites of catalyst

rls = Rate limiting step (or called that rate determining step)

CH₄-S, H₂O-S, CO-S and H₂-S = Chemisorbed CH₄, H₂O, CO and H₂, respectively

k_{CH_4} , k_{H_2O} , k_{CO} and k_{H_2} = Adsorption constant of CH_4 , H_2O , CO and H_2 , respectively

k'_{CH_4} , k'_{H_2O} , k'_{CO} and k'_{H_2} = Desorption constant of CH_4 , H_2O , CO and H_2 , respectively

k_s = Rate constant at surface of catalyst

k'_s = Reverse rate constant at surface of catalyst

For this research, the surface reaction was not in equilibrium but other reversible steps were assumed to be in equilibrium. Then, the surface reaction was irreversible and the rate limiting step as follows:



The first step (adsorption) in equilibrium:

$$r_{ads CH_4} = r_{des CH_4}$$

$$k_{CH_4} P_{CH_4} \theta_v = k'_{CH_4} \theta_{CH_4}$$

$$\theta_{CH_4} = K_{CH_4} P_{CH_4} \theta_v \quad (\text{where } K_{CH_4} = k_{CH_4} / k'_{CH_4})$$

Similarly,

$$r_{ads H_2O} = r_{des H_2O}$$

$$k_{H_2O} P_{H_2O} \theta_v = k'_{H_2O} \theta_{H_2O}$$

$$\theta_{H_2O} = K_{H_2O} P_{H_2O} \theta_v \quad (\text{where } K_{H_2O} = k_{H_2O} / k'_{H_2O})$$

The second step (surface reaction):

$$r_{rfs} = k_s \theta_{CH_4} \theta_{H_2O}$$

The third step (desorption) in equilibrium:

$$r_{ads CO} = r_{des CO}$$

$$k_{CO} P_{CO} \theta_v = k'_{CO} \theta_{CO}$$

$$\theta_{CO} = K_{CO} P_{CO} \theta_v \quad (\text{where } K_{CO} = k_{CO} / k'_{CO})$$

Similarly,

$$r_{ads H_2} = r_{des H_2}$$

$$k_{H_2} P_{H_2} \theta_v = k'_{H_2} \theta_{H_2}$$

$$\theta_{H_2} = K_{H_2} P_{H_2} \theta_v \quad (\text{where } K_{H_2} = k_{H_2} / k'_{H_2})$$

Where

θ_v = Fraction of no surface coverage on the catalyst
(void fraction)

θ_{CH_4} , θ_{H_2O} , θ_{CO} and θ_{H_2} = Fraction of surface covered CH_4 , H_2O , CO and H_2 on the catalyst, respectively

K_{CH_4} , K_{H_2O} , K_{CO} and K_{H_2} = Adsorption equilibrium constant of CH_4 , H_2O , CO and H_2 , respectively

Adding the equations for θ_{CH_4} , θ_{H_2O} , θ_{CO} , and θ_{H_2}

$$\theta_{CH_4} + \theta_{H_2O} + \theta_{CO} + \theta_{H_2} = \theta_v(K_{CH_4}P_{CH_4} + K_{H_2O}P_{H_2O} + K_{CO}P_{CO} + K_{H_2}P_{H_2})$$

Also, $\theta_{CH_4} + \theta_{H_2O} + \theta_{CO} + \theta_{H_2} + \theta_v = 1$

Hence, $1 - \theta_v = \theta_v(K_{CH_4}P_{CH_4} + K_{H_2O}P_{H_2O} + K_{CO}P_{CO} + K_{H_2}P_{H_2})$

$$\theta_v = 1 / (1 + K_{CH_4}P_{CH_4} + K_{H_2O}P_{H_2O} + K_{CO}P_{CO} + K_{H_2}P_{H_2})$$

Surface reaction, $r_{fs} = k_s\theta_{CH_4}\theta_{H_2O}$

And then $\theta_{CH_4} = K_{CH_4}P_{CH_4}\theta_v$
 $= K_{CH_4}P_{CH_4} / (1 + K_{CH_4}P_{CH_4} + K_{H_2O}P_{H_2O} + K_{CO}P_{CO} + K_{H_2}P_{H_2})$

$$\theta_{H_2O} = K_{H_2O}P_{H_2O}\theta_v$$

$$= K_{H_2O}P_{H_2O} / (1 + K_{CH_4}P_{CH_4} + K_{H_2O}P_{H_2O} + K_{CO}P_{CO} + K_{H_2}P_{H_2})$$

Thus, $-r_{CH_4} = r_{fs} = \frac{k_s K_{CH_4} P_{CH_4} K_{H_2O} P_{H_2O}}{(1 + K_{CH_4} P_{CH_4} + K_{H_2O} P_{H_2O} + K_{CO} P_{CO} + K_{H_2} P_{H_2})^2}$ (4.10)

From equation (4.10), which could be rearranged the following these conditions:

Excess steam,

$$P_{CH_4} \lll P_{H_2O}$$

$$-r_{CH_4} = r_{fs} = \frac{k_s K_{H_2O} P_{H_2O} K_{CH_4} P_{CH_4}}{(1 + K_{H_2O} P_{H_2O} + K_{CO} P_{CO} + K_{H_2} P_{H_2})^2}$$

$$= \left[\frac{K P_{H_2O}}{(1 + K_{H_2O} P_{H_2O} + K_{CO} P_{CO} + K_{H_2} P_{H_2})^2} \right] P_{CH_4}$$
 (4.11)

Where

$$K = k_s K_{CH_4} K_{H_2O}$$

Non-excess steam,

$$-r_{CH_4} = r_{fs} = \frac{k_s K_{CH_4} P_{CH_4} K_{H_2O} P_{H_2O}}{(1 + K_{CH_4} P_{CH_4} + K_{H_2O} P_{H_2O} + K_{CO} P_{CO} + K_{H_2} P_{H_2})^2}$$

$$= \frac{K P_{H_2O} P_{CH_4}}{(1 + K_{CH_4} P_{CH_4} + K_{H_2O} P_{H_2O} + K_{CO} P_{CO} + K_{H_2} P_{H_2})^2}$$
 (4.12)

Where

$$K = k_s K_{CH_4} K_{H_2O}$$

From equation (4.11) and (4.12), plot between reaction rate of methane and partial pressure of methane or steam at excess and non-excess steam, which used the experimental data from Table C4 in Appendix C, as illustrated in Figure 4.9. It was found that methane steam reforming was the first order reaction, which was consistent with Langmuir-Hinshelwood model.

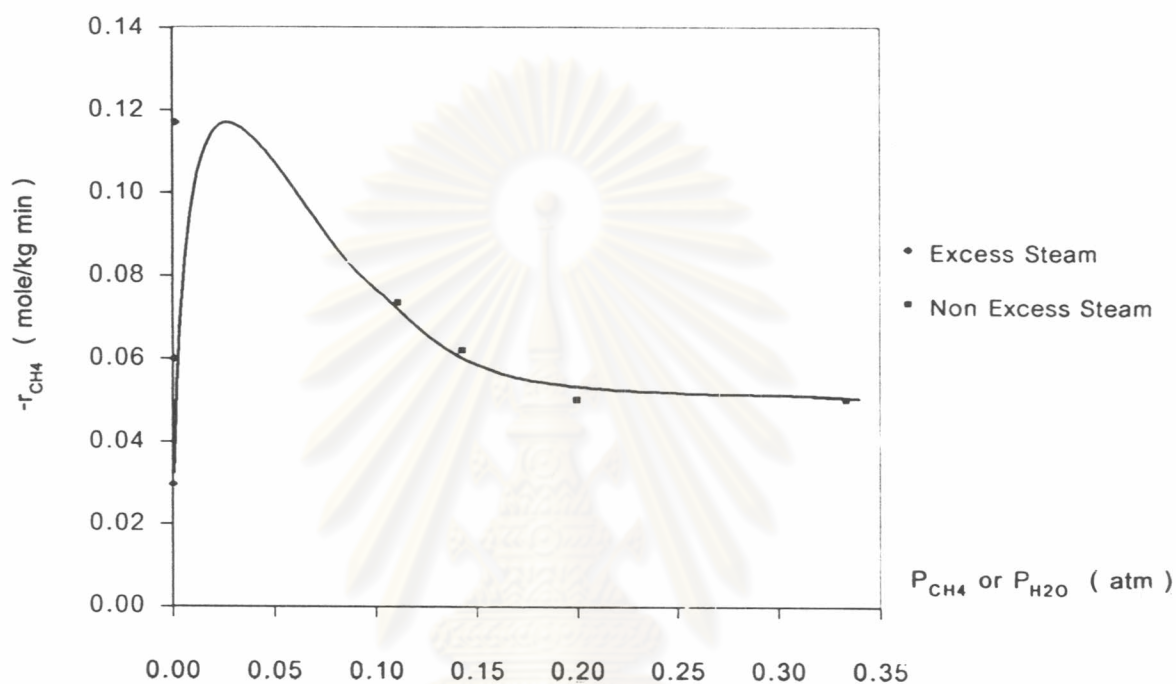


Figure 4.9. Reaction rate of methane vs. partial pressure of methane or steam at excess and non-excess steam.

4.3. The Effect of Diffusion on the Rate of Reaction

The objective of this part was to study the effect of diffusion on rate of reaction with using the criteria of Weisz and Prater. The experiment was achieved at 850 °C, steam to methane ratio from 2.0 to excess, methane feed rate from 6.0×10^{-5} to 5.1×10^{-4} mole/min, steam feed rate from 1.0×10^{-4} to 0.15 mole/min and 2 g of catalyst weight. From the criteria of Weisz and Prater, the equation could be proposed as follows:

$$\Phi = \frac{(\tau_a \rho_s)_{\text{obs}} L^2}{D_{\text{eff}} C_{\text{as}}^s} \quad (4.13)$$

From equation (4.13) it was found that if the value of Φ was considerably greater than unity then reaction was highly diffusion limitation, which was diffusion effected on rate of reaction, but if considerably smaller than unity then no diffusion limitation indicated that diffusion was no effect on rate of reaction. As a result, chemical reaction could be determined as controlling step of reaction rate. From the experimental result, Table C8 in Appendix C, found that the value of Φ was between 4.61×10^{-17} and 3.12×10^{-16} , which was considerably smaller than unity. It was indicated that chemical reaction was controlling step of reaction rate. Since the specific area of catalyst in this research was $22 \text{ m}^2/\text{g}$ less than generally used for industry about $350 \text{ m}^2/\text{g}$, internal diffusion had no effect on this reaction. This indicated that the reaction had to occur only at external surface of catalyst.

4.4. Determination of Thermodynamics Model of Reaction

The objective of this part was determination of the thermodynamics model of reaction by comparing product gas composition from the experiment with thermodynamics equilibrium at various temperatures. The experiment was achieved at $700\text{-}850 \text{ }^\circ\text{C}$, steam to methane ratio of 4.0, methane feed rate from 1.27×10^{-4} to 1.46×10^{-4} mole/min, steam feed rate from 5.07×10^{-4} to 5.86×10^{-4} mole/min and 5 g of catalyst weight. From the experimental result, Table C9 in Appendix C, it was found that the trend of product gas composition was consistent with thermodynamics equilibrium as illustrated in Figure 4.10. In addition, gas composition was above the equilibrium since it was the residual gas from the conversion, but if below the equilibrium as they were the product gases, which occurred in the reaction. Thus, the thermodynamics model of reaction could be suggested in two reactions as follows:



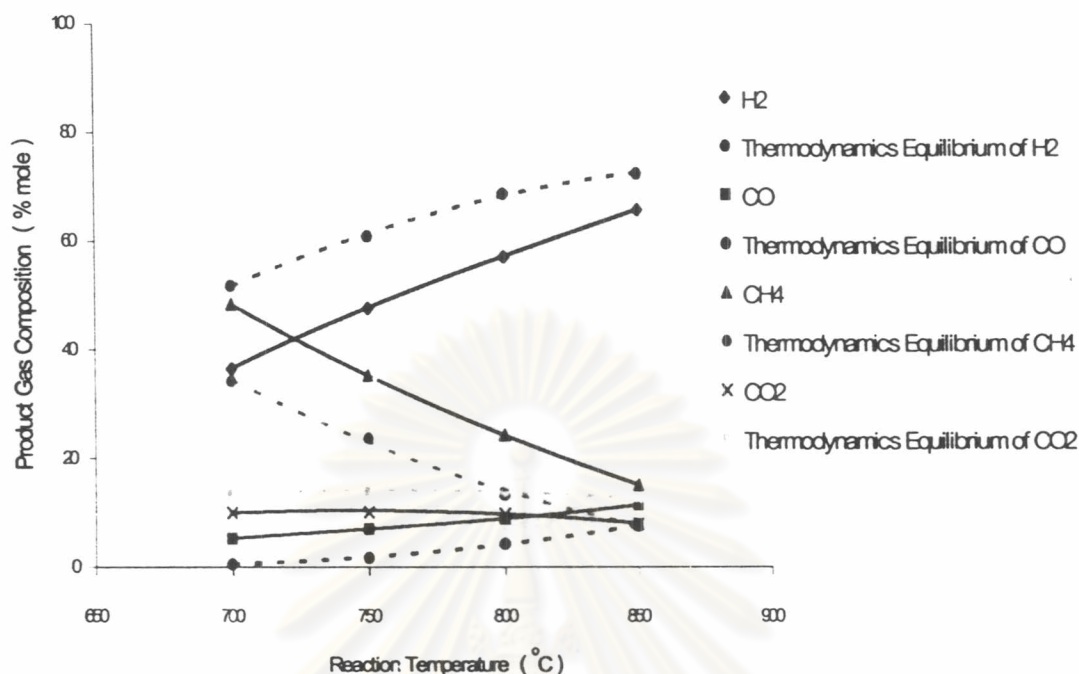


Figure 4.10. Comparison of product gas composition from the experiment with thermodynamics equilibrium at various temperatures.

4.5. Literature Comparison

For this research, the kinetics of methane steam reforming on nickel magnesia solid solution catalyst was investigated in two cases as follows:

The first, kinetics of methane steam reforming on nickel magnesia solid solution catalyst at excess steam was found that rate equation could be expressed as follows:

$$-r_{\text{CH}_4} = k P_{\text{CH}_4}$$

Where $k = 7.796 \times 10^4 \exp(-18,726.78 / RT) \text{ mole atm}^{-1} \text{ kg}^{-1} \text{ min}^{-1}$

Owing to excess steam, which was between 250 and 2400 of steam-methane ratio, it was found that activation energy was considerably greater than other literatures as illustrated in Table 4.3 because mass transfer was occurred in the reaction that methane was diffused via steam phase to surface of catalyst. Thus, order of reaction for steam had no effect on reaction rate of methane.

The second, kinetics of methane steam reforming on nickel magnesia solid solution catalyst at non-excess steam, it was found that rate equation could be expressed as follows:

$$-r_{\text{CH}_4} = k P_{\text{CH}_4} P_{\text{H}_2\text{O}}^{0.5}$$

Where $k = 2.2812 \exp(-9,041.16 / RT)$ mole atm^{-1.5} kg⁻¹ min⁻¹

Owing to non-excess steam, which was from 2.0 to 8.0 of steam-methane ratio, it was found that activation energy was considerably smaller than other literatures as illustrated in Table 4.3 because the ability of methane and steam adsorbed on the catalyst surface were similar. Thus, reaction rate of methane was dependent on order of reaction for methane and steam.

Table 4.3. Comparison of rate equation and activation energy in each literature.

Researcher	Rate Equation	Catalyst	Temp. Range (°C)	E _a (cal / mole)
Akers and Camp (1955)*	$-r_{\text{CH}_4} = k_0 e^{-E_a/RT} P_{\text{CH}_4}$	Ni/Al ₂ O ₃	337-637	8,820
Rostrup-Nielsen (1975)*	$-r_{\text{CH}_4} = k_0 e^{-E_a/RT} [P_{\text{CH}_4}(1-(Q_r/K_p))]$	Ni/SiO ₂ -Al ₂ O ₃	500-680	11,165
Vitidsant (1988)*	$-r_{\text{CH}_4} = k_0 e^{-E_a/RT} C_{\text{CH}_4}$	Ni/Al ₂ O ₃	600-850	12,518
Thaneerat (1994)*	$-r_{\text{CH}_4} = k_0 e^{-E_a/RT} C_{\text{CH}_4}^{1.119} C_{\text{H}_2\text{O}}^{0.385} C_{\text{CO}_2}^{-1.311}$	Ni/Al ₂ O ₃	550-700	15,149
This work (2003)				
a) Excess steam	a) $-r_{\text{CH}_4} = k_0 e^{-E_a/RT} P_{\text{CH}_4}$	Ni _{0.03} Mg _{0.97} O	700-850	18,727
b) Non-excess steam	b) $-r_{\text{CH}_4} = k_0 e^{-E_a/RT} P_{\text{CH}_4} P_{\text{H}_2\text{O}}^{0.5}$			9,041

* Non-excess steam condition

From Table 4.3, this work was less activation energy at non-excess steam than the work's Rostrup-Nielsen, Vitidsant and Thaneerat. As a result, the reaction rate in this work was higher. Besides, this activation energy was higher than the work of Akers and Camp that enabled lower reaction rate of this work. These results were caused by different conditions such as temperature and catalyst.